EGYPTIAN ACADEMIC JOURNAL OF
BIOLOGICAL SCIENCES
D
HISTOLOGY & HISTOCHEMISTRY

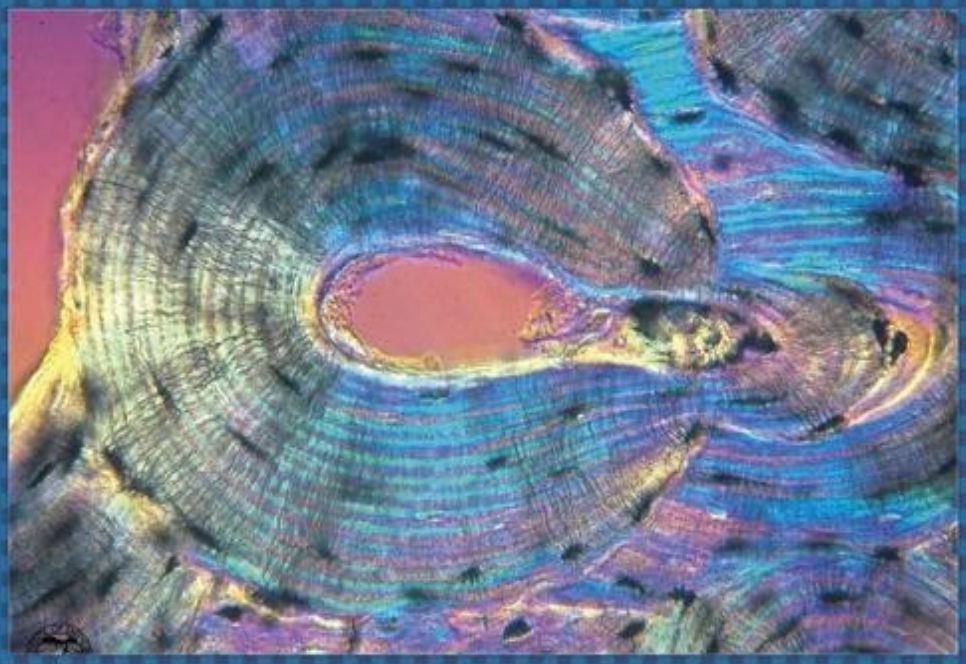

ISSN
2090-0775

WWW.EAJBS.EG.NET

Vol. 17 No. 2 (2025)

Citation: Egypt. *Acad. J. Biolog. Sci. (D-Histology and histochemistry) Vol.17(2) pp1-20(2025)*
DOI: 10.21608/EAJBSD.2025.447079

Egypt. Acad. J. Biolog. Sci., 17(2):1-20 (2025)

Egyptian Academic Journal of Biological Sciences
D. Histology & Histochemistry
ISSN 2090 – 0775
http://eajbsd.journals.ekb.eg

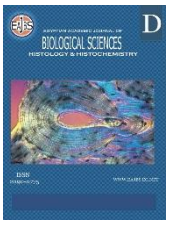

The Possible Protective Role of Hesperidin Versus Acrylamide-Induced Neurotoxic Effects on the Prefrontal Cortex of The Adult Male Albino Rat

Hala M. Hassanin; Mohamed El-Badry; Reham R. Abd Elhafiz and Noha A. Rashed

Department of Human Anatomy and Embryology, Faculty of Medicine, Assiut University, Egypt.

E-mail : noharashed@aun.edu.eg

ARTICLE INFO

Article History
Received:4/7/2025
Accepted:12/8/2025
Available:16/8/2025

***Keywords*:**
Hesperidin Reduces Acrylamide Toxic Effects On Rat Prefrontal Cortex.

ABSTRACT

Background: Numerous harmful consequences appeared-with appearance of acrylamide (AC) in our daily consuming products. Hesperidin (Hs) is a flavone glycoside that is commonly used as anti-inflammatory agent. **Aim of the Work:** to offer an experimental foundation for prevention and reduction of acrylamide poisoning using hesperidin. **Material and Methods**: 40 adult male albino rats were divided into four groups: Control group (I), Hs treated group (II) with a dose of 10 mg/ kg B. W. /day. Hs was dissolved in 0.1% carboxy methyl cellulose, AC treated group (III) with a dose of 25 mg/kg B. W. /day and AC-Hs group (IV) received the same doses as Group II and Group III. All treatments were given orally via gavage for 21- consecutive days. At the end of experiment, prefrontal cortices were extracted and processed for the light, electron microscopic examination and immunohistochemical staining. Morphometric measurements were also done. **Results:** AC treated group revealed hemorrhage and congestion in both cortical blood vessels and pia mater. Pyramidal cells were shrunken with pyknotic nuclei, pericellular halos and loss of their processes. The granule cells were affected and showed ill-defined boundaries and lost their nuclei. The morphometric studies revealed a significant decrease in body weight and mPFC thickness of AC treated rats. On the other hand, rats received hesperidin with acrylamide revealed more or less apparent normal architecture as control group. **Conclusion:** Treatment with hesperidin is able to attenuate acrylamide induced brain damage in the rats.

INTRODUCTION

Several aspects of social behavior in animals, including recognition, social motivation, and decision-making, depend on the prefrontal cortex (PFC) (Mohapatra & Wagner, 2023). PFC is situated in the frontal lobe, anterior to the premotor cortex and primary motor cortex, and it comprises approximately 29% of the total cerebral cortex (Kolk & Rakic, 2O22). The PFC is made up of three parts: the orbital prefrontal cortex (also known as the orbitofrontal cortex), the medial prefrontal cortex, and the lateral prefrontal cortex (Córcoles-Parada *et al., 2017*).

Three topologically distinct areas normally make up the rat prefrontal cortex. First, the bulk of the cerebral hemisphere's medial wall is composed of the medial prefrontal cortex, which is situated medially and dorsally to the genu of corpus callosum. Second, the anterior part of the rhinal sulcus in rats has a laterally positioned cortical region called the lateral (sulcal PFC), also referred to as the agranular insular cortex.

The third is the orbital prefrontal cortex, which is located ventrally in the posterior region of the rhinal sulcus, somewhat posterior to the caudal end of the olfactory bulb (Heidbreder & Groenewegen, 2003).

Most prefrontal regions in human consist of six layers, which include the fourth layer (internal granular layer); but the rat cortical limbic system includes the posterior orbitofrontal and medial PFC, which is formed of fewer than six layers (García-Cabezas *et al.,* 2019).Acrylamide(AC), which has the chemical formula C3H5NO, is a reactive α, β-unsaturated (conjugated) molecule (Shukor, 2019).

Acrylamide was accidentally discovered in 2002 to be present in food rich in starch, including fries, bread, chips, biscuits and food cooked at very high temperatures, either by baking or frying (Sabo *et al.,* 2021). The Maillard reaction in processed food is the primary cause of AC exposure in humans (Zamani *et al.,* 2018). Prior to its discovery in food, AC was a well-known industrial chemical substance that was mostly utilized as a building block in several industrial processes, as the manufacturing of paper, glues, plastics, cigarette smoke, and drinking and wastewater treatment, Additionally, waterproofing sealing gel contains acrylamide (Rifai & Saleh, 2020).

Acrylamide exposure has been linked to several health risks in both human and animal models, including genotoxicity, hepatotoxicity, carcinogenicity, and reproductive toxicity in animal models (Zouhairi *et al.,* 2022). Acrylamide exposure causes neurotoxicity in humans, which is manifested by polyneuropathy, weight loss, ataxia, weakness of skeletal muscle, fatigue, and numbness in hands and feet (Park *et al.*, 2021).Hesperidin (Hs) is one of the flavanone glycosides that occurs naturally in citrus fruits (Küçükler *et al.,* 2021), that has many biological benefits because of its anti-inflammatory and antioxidant qualities in models of cardiovascular diseases (Parhiz *et al.,* 2015). It helps in the management of inflammation-induced damage to the liver and renal tissue (Turk *et al.,* 2019) and cancer prevention (Roohbakhsh *et al.*, 2015).

Hesperidin's anti-inflammatory effects and antioxidant properties help to decrease symptoms in animal models of Alzheimer's disease and other neurodegenerative illnesses (Sawikr *et al.,* 2017), Parkinson's disease (Jung & Kim, 2018), neuro-immunological multiple sclerosis (MS) (Haghmorad *et al.,* 2017) and traumatic injuries to the central nervous system and brain damage caused by a lack of blood flow (Kosari-Nasab *et al.,* 2018).

So, the aim of this study is to offer an experimental foundation for prevention and treatment of acrylamide poisoning using hesperidin.

MATERIALS AND METHODS

Chemicals:

Acrylamide with a purity 99.9% and Hesperidin bought from the chemical company Sigma-Aldrich.

Experimental Animals:

In this experiment, forty mature three-month-old male albino rats were employed. These animals were purchased from the Assiut University of Egypt's Faculty of Medicine's Animal House. The animals were housed individually in wire mesh cages with natural ventilation at room temperature. They were given water and regular laboratory food. Every experimental method was carried out in accordance with the Faculty of Medicine's Ethics Committee Guidelines, with ethical permission number (17101763) Assiut University, Egypt.

Experimental Design:

The rats in this experiment were randomly assigned to four groups of ten rats each.

1. **Group I (Control group**), rats in this group received only standard food and water adlibitum for studying the normal structure of prefrontal cortex.

2. **Group II (Hs group),** rats received Hs only in a dose of 10 mg/ kg B W /day. Hs was dissolved in 0.1% carboxy methyl cellulose according to (Elhelaly *et al.,* 2019).
3. **Group III (AC group),** rats received acrylamide in a dose of 25 mg/kg B W /day. Before being used, AC was dissolved in a saline solution according to (Gedik *et al.,* 2017).
4. **Group IV (AC-Hs group),** Hs was co-administrated with Ac in the same doses as Group II and Group III.

All treatments were administered once daily at the same hour for 21 succeeding days, via a tube inserted through the mouth. The rats were anesthetized by an ether inhalation then we opened rats' chests with exposure to a left ventricular intracardiac perfusion using normal saline (0.9% NaCl) and 4% paraformaldehyde solution. The perfusion persisted until the right atrial venous return was clear. Then, the rats' skulls were fixed in 10% formalin for 10 days. Afterwards, the prefrontal cortices were extracted, cut into small pieces and fixed in 10% formalin for (light microscopy) and 2.5 % cold glutaraldehyde (for electron microscopy) and processed for histopathological analysis.

Histological Study:

Light Microscopic Study:

After being sliced to the proper size and shape, the fixed tissues were placed into the embedding cassettes. Then placed in increasing alcohol grades to dehydrate them, samples were embedded in blocks of paraffin (5-7 um), paraffin blocks were cut and trimmed. After three minutes in hematoxyline solution, the slides were rinsed with distilled water. Following eight dips with acetic acid, the slides were soaked in ammonium hydroxide. Dehydration was done in increasing ethanol grades. The slides were immersed in eosin for one minute and then dehydrated again in 100% ethanol. After mounting them in Per mount media, coverslips were added (Suvarna *et al.,* 2018). The stained slides were examined in the Department of Human Anatomy and Embryology, Faculty of Medicine, Assiut University, using an optical microscope (OLYMPUS CX31-Japan).

Electron Microscopic Study:

The tissues were chopped into pieces that were about 1 mm by 1 mm. The main fixation process was then carried out for two hours at room temperature in 2.5% glutaraldehyde + 4% formaldehyde, post-fixative osmium tetroxide, dehydration (by increasing alcohol grades), infiltration (by Epon araldite), embedding in new resin, and preparation of semi-thin sections of 0.5-1 um using an Assiut University ultramicrotome. The sections underwent toluidine blue staining, light microscopy examination, and photography.

Ultrathin pieces (50–80 nm) were cut from particular areas of the mPFC (layer 5) of the trimmed blocks and gathered on a copper grid. The ultrathin slices have been analyzed using uranyl acetate and lead citrate under transmission electron microscopy (Woods & Stirling, 2018). An electronic microscopic examination was performed with modest magnification initially to find the specimen, then a larger one to identify the cells. A transmission electron microscope (TEM) ("Joel" E.M.-100 CX11; Japan) was used to photograph and examine the stained ultrathin sections at Assiut University's Electron Microscopic Unit.

Immunohistochemical Study:

Following formalin fixation, brain samples were hydrated following deparaffinization on charged slides and stained immunohistochemically using the avidin–biotin peroxidase technique. The sections have a thickness of 5 μm. They utilized 0.01 mol/l citrate buffer (PH 6.0) to expose the antigen. Thermo Scientific Company, USA's 1:100 monoclonal mouse anti-GFAP was then used as the main antibody, was incubated, followed by hydrogen peroxide, followed by biotinylated secondary antibodies and 0.05% diaminobenzidine. Followed by streptavidin-biotin complex incubation

after being cleaned with phosphate buffer saline (PBS) and biotinylated secondary antibodies. To visualize the reactions, 0.05% DAB was used as a chromogen. After being dehydrated, cleaned, and mounted, the slides were counter-stained with Myer's haematoxylin. The nuclei were blue and the positive cells brown (Abdel-aziz *et al.,* 2019).

Morphometric Study and Statistical Analysis:

Rats in each group had their body weight (BW) measured at the start and finish of the trial. To estimate the thickness of the medial prefrontal cortex a line drawn from the central sulcus to the gray-white matter transition zone at a magnification of 100 was used. The measurements were taken at Assiut University's Faculty of Medicine's Anatomy Department using the Leica Q500 image analyzer. In ten randomly selected fields 10 recordings were acquired for each group.

The SPSS software (version 16) was used to gather, edit, and statistically analyze the data using analysis of variance (ANOVA) and Tukey's post hoc test. The computed mean value ± standard deviation was used to express the data. If the probability value, often known as the p-value, was less than 0.05, it was deemed significant.

RESULTS

Histological Results:

A-Light Microscopic Results:

Hematoxyline and Eosin – Stained Results:

Group 1 (control group): The layers of the medial prefrontal cortex were revealed by examining sections of the control animals' prefrontal cortex stained with hematoxylin and eosin. From the outside in, these 5 ordered layers were, the molecular layer, the outer granular layer, the outer pyramidal layer, the inner pyramidal layer, and finally the multiform layer. The medial prefrontal cortex lacked the fourth layer, often known as the inner granular layer (Fig. 1a). In reference to the third layer, also known as the outer pyramidal layer, medium-sized pyramidal cells with granular cells displayed big, rounded nuclei (Fig. 2a). There were a few granular cells with big rounded vesicular nuclei and limited perivascular space around the blood vessels, but the majority of the cells in the fifth layer (inner pyramidal layer) were huge pyramidal cells with apical long processes and vesicular nuclei (Fig. 3a).

Group 2 (Hesperidin- treated group): Analysis of the hesperidin-treated animals hematoxyline and eosin-stained medial PFC sections revealed that the layers were arranged normally, resembling the control group in that they had five ordered layers with normal blood vessels, a normal perivascular space, and a normal attached pia matter (Fig. 1b). Medium-sized pyramidal cells with vesicular nuclei, apical long processes, also granular cells exhibited big, rounded vesicular nuclei in the outer pyramidal layer (Fig. 2b). Large pyramidal cells with apical long processes and vesicular nuclei accounted for the majority of the cells in the hesperidin group (inner pyramidal layer), but a small number of granular cells with big rounded vesicular nuclei were also present (Fig.3b).

Group 3 (Acrylamide- treated group): The medial prefrontal cortex of the acrylamide-treated animals was examined under a microscope after staining with hematoxylin and eosin, which showed marked abnormal changes in the histological appearance of the medial Prefrontal cortex. It displayed pia mater hemorrhage and congestion together with perivascular and cellular infiltration. Cortical blood vessels were also noted (Fig. 1c). Shrunken tiny pyramidal cells with lost processes were visible in the exterior pyramidal layer. The perivascular area around blood vessels was also seen, along with granular cells that lacked nuclei and had poorly defined cell borders (Fig. 2c). Pyramidal cells with a more or less typical form and strongly stained nuclei encircled by vacuoles and pericellular halos were seen in the internal pyramidal layer (Fig. 3c).

Group 4 (Acrylamide – Hesperidin treated group): Sections of the prefrontal cortex of the rats treated with acrylamide and hesperidin that were stained with hematoxyline and eosin appeared to have a normal organization of cerebral layers, with only little congestion and pia matter separation (Fig. 1d). Some medium-sized pyramidal cells with vesicular nuclei and long apical processes were visible in the outer pyramidal layer, whereas a small number had shrunken and heavily discolored nuclei. Granule cells had vesicular nuclei and were normal (Fig. 2d). Some strongly pigmented, pyknotic cells with vacuolation encircling them were visible in the inner pyramidal layer, whereas other pyramidal cells with vesicular nuclei and apical long processes seemed normal. With vesicular nuclei like those of the control group, granule cells seemed to be normal (Fig. 3d).

Toluidine Blue-Stained Results:

Group 1 (control group): Intact pyramidal neurons with open-faced nuclei encircled by pale cytoplasm, basophilic Nissl granules, and intact long apical dendrites were seen in semi-thin slices of the prefrontal cortex from control rats that were stained with toluidine blue. Additionally, it had normal blood vessels inside an intact neuropil, normal granular cells with vesicular nuclei, and normal perineural neuroglia with rounded nuclei (Fig. 4a).

Group (3) Acrylamide–treated group revealed deformed, pyknotic and deeply stained pyramidal cells with irregular cell bodies and axons, many vacuoles appeared in the neuropil, perineural neuroglia beside the degenerated neuron, distorted granular cell with ill-defined borders and lost their nuclei (Fig. 4b).

Group (4) AC-Hs treated group seemed improved as compared to group III. Some of the pyramidal cells had strongly pigmented nuclei encircled by vacuolation, while others had vesicular nuclei encircled by pale cytoplasm containing basophilic Nissl granules with long intact processes. The granular cell resembled the control group in most aspects. Blood vessels that were situated in the surrounding neuropil and had noticeable perivascular gaps. Glial cells and perineural glial cells were seen next to both affected and healthy neurons (Fig. 4c).

B=Electron Microscopic Results:

Group 1 (control group): The control group's pyramidal cells were examined on ultrathin sections and revealed a big vesicular nucleus, a conspicuous nucleolus, and apical dendrites with normal histological structure. Within an intact neuropil, their cytoplasm had normal mitochondria and a normal rough endoplasmic reticulum (Fig.5a). Large, rounded nuclei and normal mitochondria and rER were present in the granular cells (Fig. 6a). With compact, consistent myelin lamellae and a smooth, regular shape that displayed normal mitochondria, myelinated fibers seemed normal (Fig. 7a).

Group 3 (AC treated group): On ultrathin examination of the acrylamide–treated group pyramidal cells appeared shrunken, their nuclei exhibited nuclear membrane infoldings and condensation of chromatin and dilated rER in the cytoplasm. The cytoplasm showed damaged mitochondria, many vacuolation and irregular outlines of myelinated axon (Fig.5b). The granular cells were apparently reduced in size and revealed invagination of the nuclear membrane and chromatin condensation. The cytoplasm contained irregularly myelinated axons with swollen and shrunken mitochondria and perineural neuroglial cells beside the granular cell (Fig. 6b). The myelinated axons exhibited an irregular outline with focal interruption and revealed that the myelin sheaths splitting. The axoplasm was found to contain vacuoles and damaged mitochondria (Fig. 7b).

Group 4 (AC-Hs treated group): On ultrathin examination of Group IV acrylamide – hesperidin treated group showed most of the pyramidal cells appeared with normal nucleus, prominent nucleolus, apical dendrites, nuclear membrane apparently normal

without invagination or splitting, the pyramidal cell surrounded by perineural neuroglial cell, normal mitochondria and slightly dilated rough endoplasmic reticulum. (Fig. 5c). The granular cells appeared normal and had similar structure to the control group with vesicular nuclei, regular contour, normal nuclear membrane without invagination nor splitting and the cytoplasm showed intact rounded mitochondria (Fig. 6c).

Regular myelin sheaths encased the majority of myelinated nerve fibers with normal mitochondria. Few of the myelinated nerves showed disrupted mitochondria (Fig. 7c).

C-Immunohistochemical stained results:

Group 1 (control group): The control group showed very few astrocytes with short, thin few processes that reacted positively to the GFAP immune-histochemical staining (Fig. 8a)

Group 3 (AC treated group): When compared to the control group, the acrylamide-treated group's GFAP immunohistochemical staining revealed a greater expression of GFAP-positive cells, which appeared to have increased in number, size, and intensity. These cells also had many long, thick, branched cytoplasmic processes (Fig. 8b).

Group 4 (AC-Hs treated group): The amount of GFAP- positive immunoreactive astrocytes of the Acrylamide-hesperidin group's that showed up with thin, less branching processes throughout the layers of the medial prefrontal cortex appeared to appeared to have decreased (Fig. 8c).

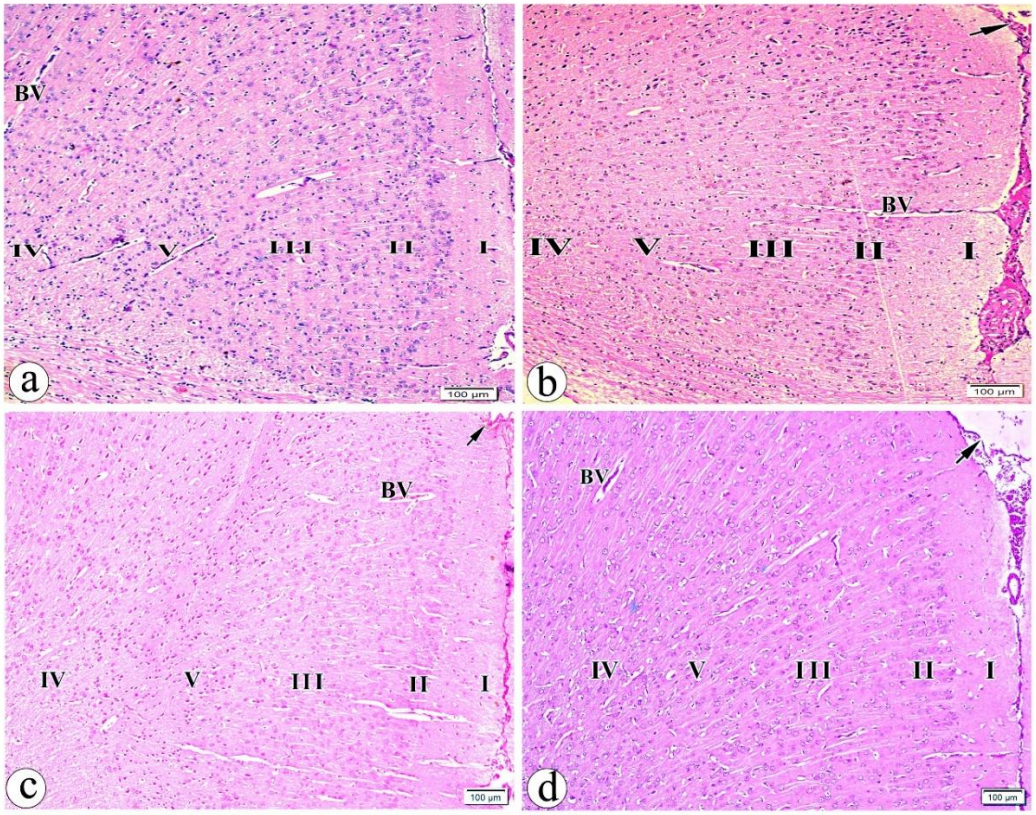

Fig. (1): Photomicrographs of a coronal section of the adult male albino rat's medial prefrontal cortex showing that **(a) the control** cerebral molecular layers (I) are arranged normally, followed by the outer granular layer (II), The outer pyramidal layer (III), the inner pyramidal layer (V), the multiform layer (IV), and the normal blood vessels (BV). **(b) The group treated with hesperidin** exhibited typical cerebral cortex layer organization, with normal blood vessels (BV) and pia matter (short arrow) connected**. (c) The group treated with acrylamide** exhibits dilated blood vessels (BV), separation of pia matter (short arrow), and disorganized cerebral cortex layers especially in layer II and III. **(d) The group treated with acrylamide and hesperidin** reveals normal blood vessels (BV), slight separation of the pia matter (short arrow), and an apparently normal arrangement of brain layers. **(hematoxyline and eosin, X100, scale bar100um).**

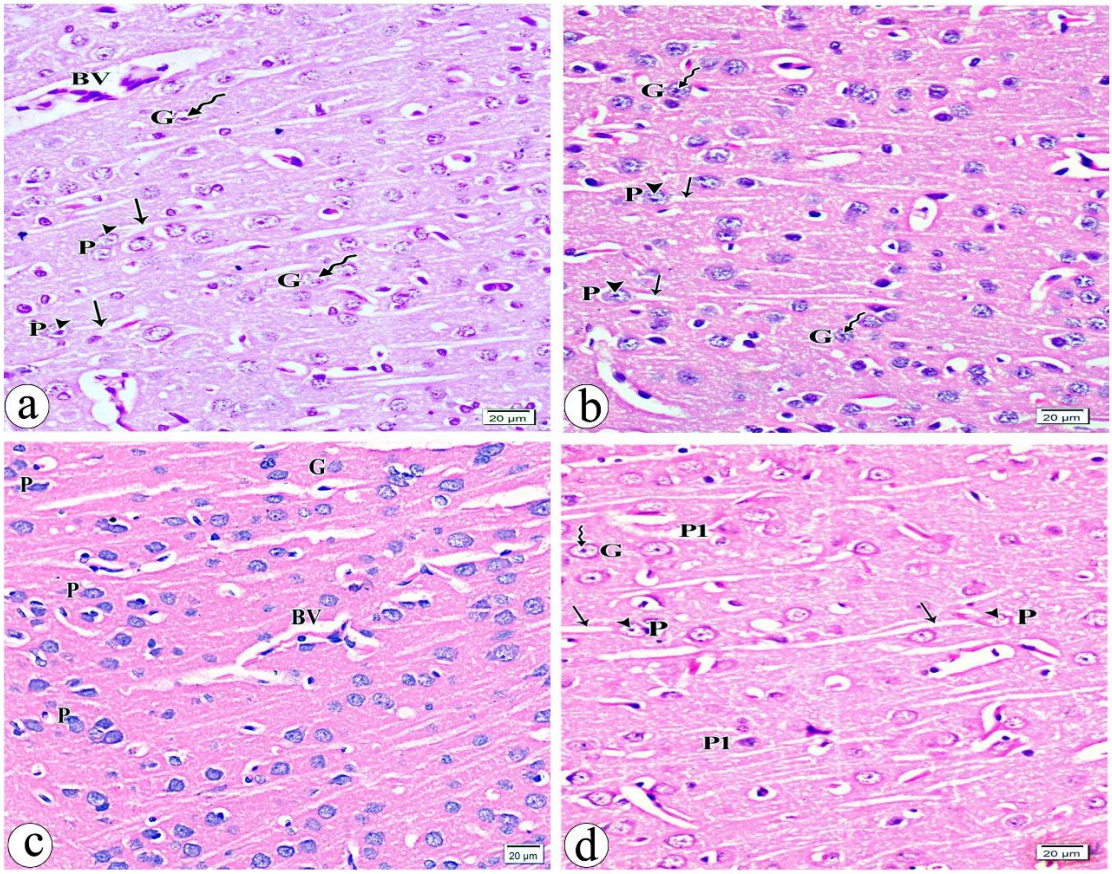

Fig. (2): Photomicrographs of the outer pyramidal layer III of medial prefrontal cortex coronal section of the adult male albino rat group **(a) control group** displaying granular cell (G) with large rounded vesicular nuclei (wavy arrows), blood vessels with normal perivascular space (BV), and medium sized pyramidal cell (P) with vesicular nuclei (arrowheads) and long apical dendrites (arrows). **(b)** The outer pyramidal layer (III) of **the Hesperidin group** has medium-sized pyramidal cells (P) with long apical dendrites (arrows) and vesicular nuclei (arrowheads). Additionally, visible are granular cells (G) with large, rounded vesicular nuclei (wavy arrows). **(c) The acrylamide group** shows a pyramidal cell (P) that has shrunk and lost its processes. Blood vessels (BV) are surrounded by a broad perivascular space, while granular cells (G) lose their nuclei and have an unclear cell border. **(d) The acrylamide-hesperidin group** displays a medium-sized pyramidal cell (P) with long apical dendrites (arrows) and vesicular nuclei (arrow heads). Additionally, some pyramidal cells appear shrunken with pyknotic nuclei that are deeply stained (P1), and granular cells (G) contain large, rounded vesicular nuclei (wavy arrow).

(hematoxyline and eosin, X 400, scale bar 20um).

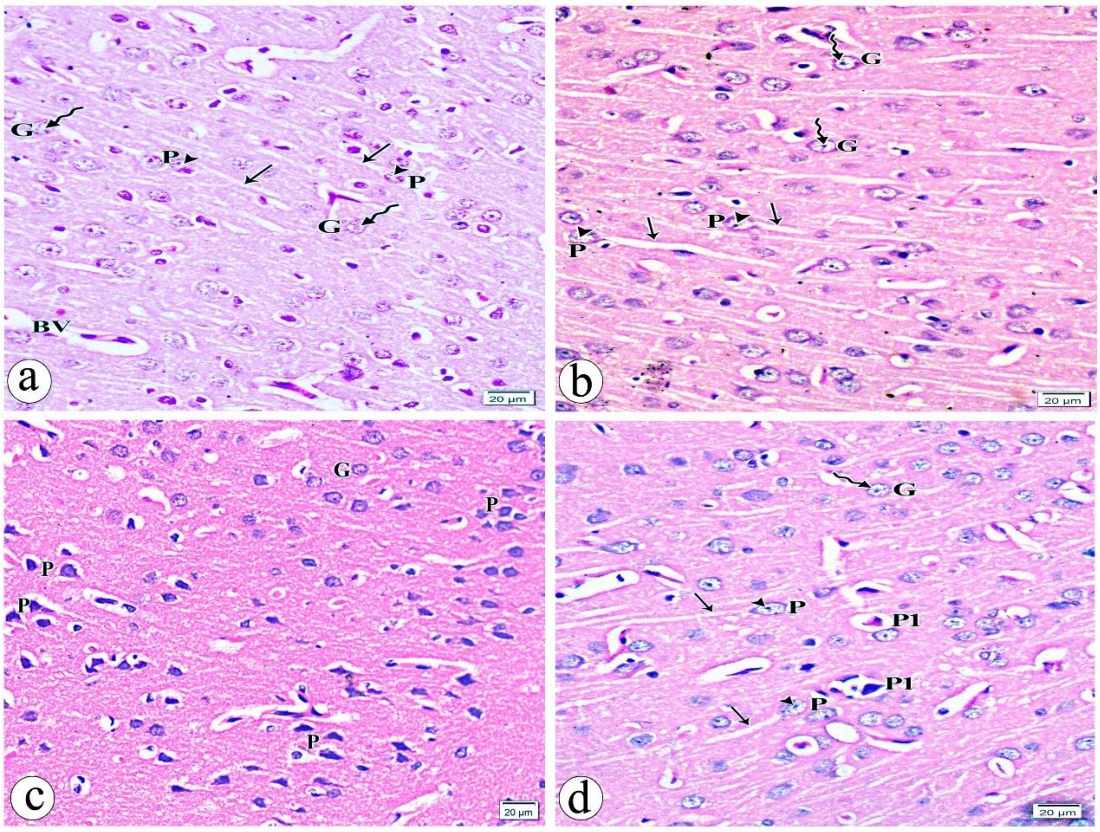

Fig. (3): Photomicrographs of the coronal section in medial prefrontal cortex (mPFC) of the inner pyramidal layer, layer V of the adult male albino rat demonstrating **(a) the control group**, which includes granular cells (G) with large rounded vesicular nuclei (wavy arrows), blood vessels with normal perivascular space (BV), and large pyramidal cells (P) with vesicular nuclei (arrow heads) and long apical dendrites (arrows). **(b) The Hesperidin group** displays granular cells (G) with big rounded vesicular nuclei (wavy arrows) and huge pyramidal cell (P) with vesicular nuclei (arrowheads) and lengthy apical dendrites (arrows). **(c) The pyramidal cell (p) in the acrylamide group** has a shrunken nucleus and lost its processes. The vacuolar spaces surrounding the pyramidal cells. the granular cell (G) in this layer appears to have lost their nuclei, with an unclear boundary. **(d)Acrylamide-hesperidin group:** The granular cell (G) has large rounded vesicular nuclei (wavy arrow), while some pyramidal cells (P) are large with vesicular nuclei (arrowhead) and long apical dendrites (arrow)while other shows some shrunken, pyknotic pyramidal cells (P1) with loss of their processes and vacuolar spaces surrounding them.

(hematoxyline and eosin, X400, scale bar 20um).

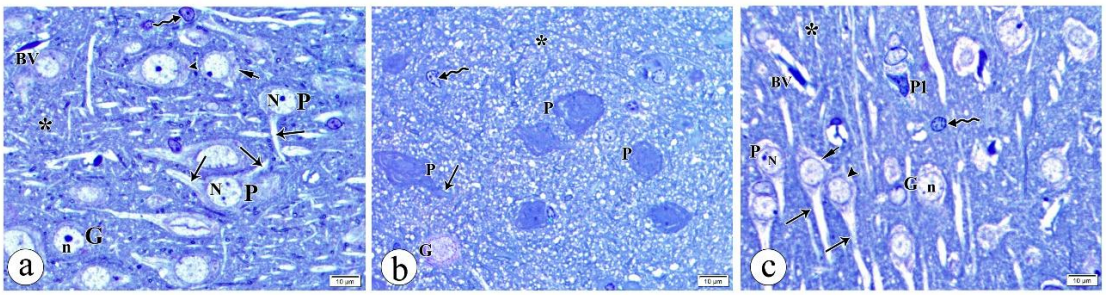

Fig. (4): Photomicrographs of toluidine blue-stained semithin medial PFC sections in the adult male albino rat showing layer V of the **(a) control group** revealing intact pyramidal cell (P) with open-faced nuclei (N) surrounded by pale cytoplasm (short arrow) that have intact long apical dendrites (arrow) and basophilic Nissl granules (arrowhead). It also displays normal granular cell (G) with vesicular nucleus (n), perineural neuroglial cells with sharply rounded nuclei (wavy arrow), and normal blood vessels (BV) that are seen within an intact neuropile (*). **(b) The group treated with acrylamide** has a deformed pyramidal cell (P) that is shrunken, has deeply discolored outlines, an uneven cell body, and aberrant apical dendrites (arrow), Alongside the degenerated neuron (wavy arrow), there are several vacuolations in the neuropil (*) and perineural neuroglia. Granular cells (G) have irregular shapes and have lost their nuclei. **(c) The AC-Hs treated group** displays an apparently normal pyramidal cell (P) with open faced nuclei (N) surrounded by pale cytoplasm (short arrow) and basophilic Nissl granules (arrowhead) with long intact apical dendrites (arrow). Perineural neuroglia (wavy arrow) appear next to the shrunken degenerated pyramidal cell (P1), granular cell (G) more or less resembles the control group with rounded vesicular nucleus (n) within apparently intact neuropil (*), and apparently normal blood vessels (BV).

(Toluidine blue x 1000, scale bar 10um).

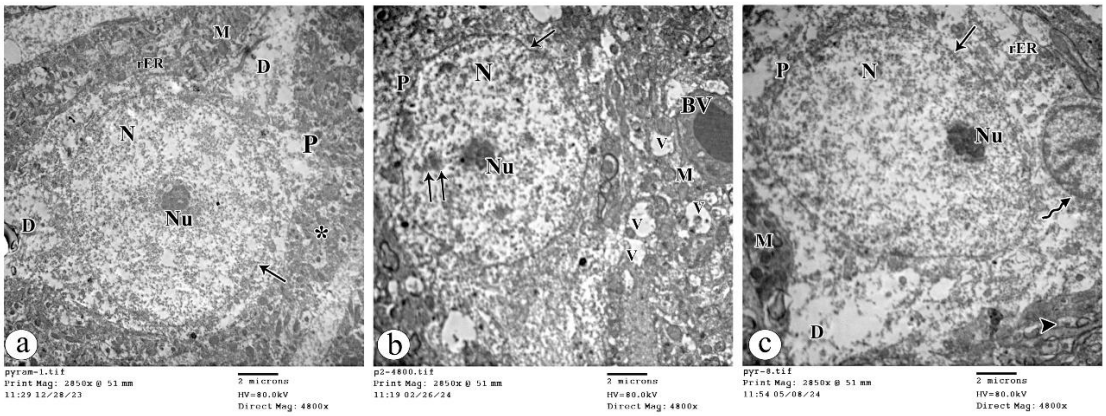

Fig (5): Electron micrographs of pyramidal cells (P) in the medial PFC of adult male albino rat showing (a) **the control group** revealing vesicular nucleus (N), prominent nucleolus (Nu), apical dendrite (D), intact nuclear membrane (arrow), intact mitochondria (M), and normal rough endoplasmic reticulum (rER) within an intact neuropile (*). **(b) The AC-treated group** exhibits nuclear membrane invagination (arrow), a condensed chromatin fragment (double arrow), a conspicuous nucleolus (Nu), and a shrunken nucleus (N). Vacuolation (V), damaged mitochondria (M), and dilated, clogged blood vessels (BV) around the pyramidal cell. **(c) The group treated with AC-Hs,** reveals Pyramidal cells with a rounded euchromatic nucleus (N), a conspicuous nucleolus (Nu), an apical dendrite (D), and an apparently normal nuclear membrane (arrow), surrounded by perineural neuroglial cell (wavy arrow) slightly dilated rough endoplasmic reticulum (rER), apparently normal myelinated axon (arrowhead) and apparently normal mitochondria (M). **(TEM x 4800).**

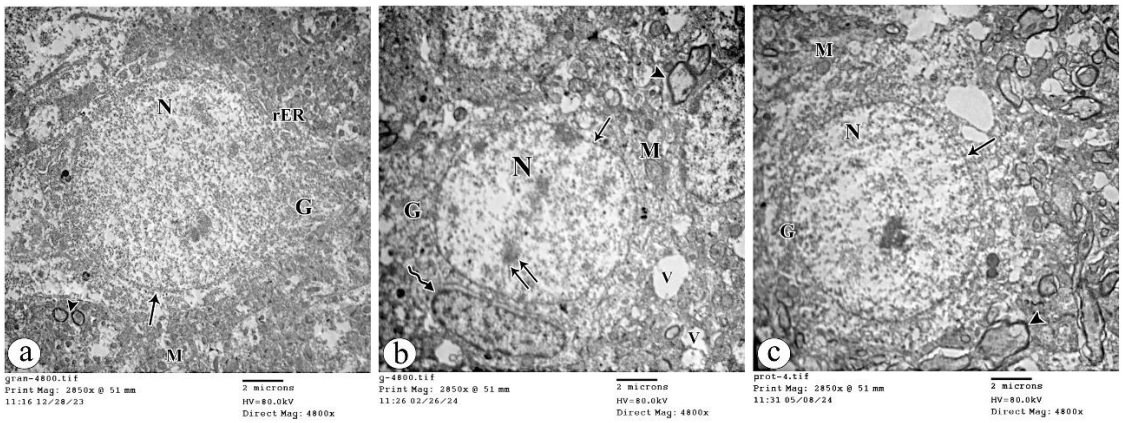

Fig. (6): Electron micrographs of granular cells **(G)** in the mPFC of adult male albino rats **(a) control group** reveals granular cells (G) with a vesicular nucleus (N), intact mitochondria (M), a normal rough endoplasmic reticulum (rER), and a normal myelinated neuron (arrow head) **(b) Granular cell in AC-treated group** (G) with shrunken nucleus (N), nuclear membrane invagination (arrow), chromatin condensation (double arrow), granular cell encircled by vacuolation (V), and peri-neuronal glial cell (wavy arrow) next to it. Additionally visible are the balloon-shaped mitochondria (M) and the asymmetrical myelinated axon (arrowhead). **(c)The AC-Hs-treated group** displaying Granule cells (G) with vesicular nuclei (N) and normal nuclear membranes (arrow), seemingly normal myelinated axons (arrowhead), and rounded, undamaged mitochondria (M). **(TEM X4800).**

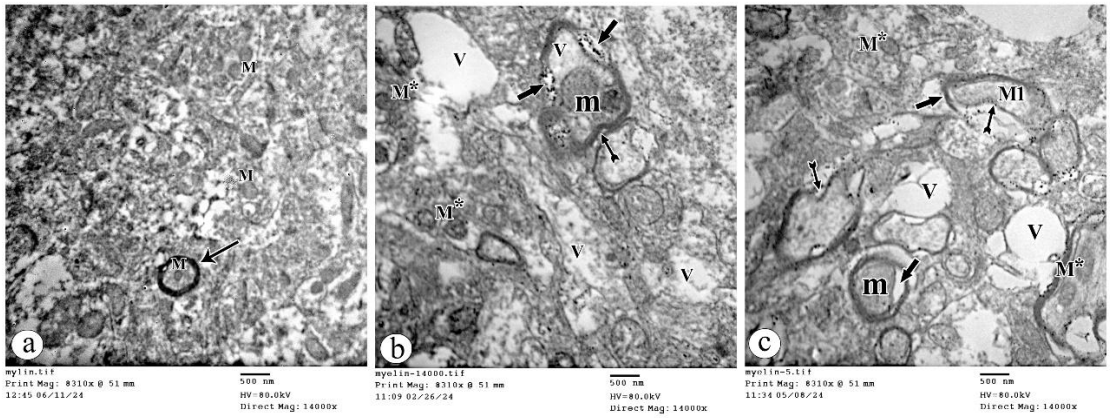

Fig. (7): The adult male albino rat's (mPFC) electron micrographs of myelinated axon in **(a) The control group** displaying normal mitochondria (M) and a smooth, regular contour with regular myelin lamellar arrangement (arrow). **(b) The AC-treated group** revealing myelin lamellae splitting (thick arrow), cytoplasmic vacuoles (V) and enlarged mitochondria (m), as well as irregular outlines with localized interruption (tailed arrow) encircled by damaged mitochondria (M*) and vacuolation (V). **(c) The myelin sheath of the AC-Hs treated group** seems intact, with the exception of the thick arrow (region of myelin lamellae splitting) and the tailed arrow (area of invagination) encircled by vacuolation (V). There are several types of mitochondria: some of them are ballooned (m), disturbed (M1) and (M*) more or less similar to control group.

(TEM X 14000).

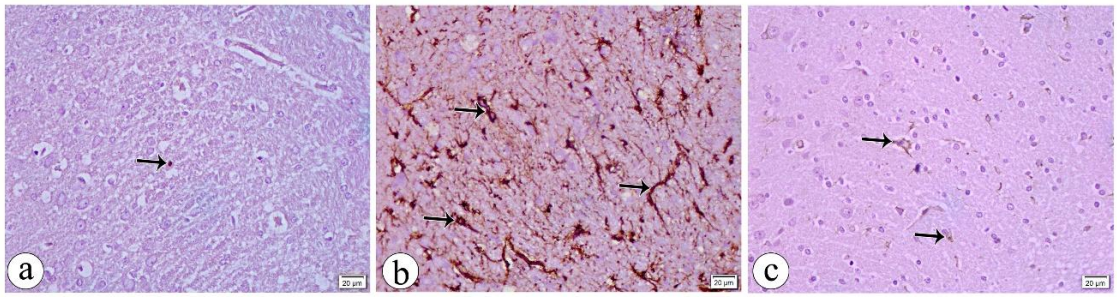

Fig (8): photomicrographs of GFAP-immunostained coronal slices in the mPFC of an adult male albino rat **(a) control group** reveals a small number of GFAP-positive immunoreactive astrocytes (arrow) with short, thin few processes. (b) **the AC group** when compared to the control one displays GFAP-positive cells (arrow) that are larger, more numerous, and more intense, along with a large number of thickly branched, lengthy cytoplasmic processes. **(c) The AC-Hs group** shows narrow, less branching processes and seems to have less GFAP-positive immunoreactive astrocytes (arrow).

(Anti GFAP X 400, scale bar 20um)

Morphometric Results:

Body Weight:

Rats in group III (the Acrylamide-treated group) had a statistically significant decreased body weight (BW) than rats in groups I and II (P = 0.001). When compared to group III (Acrylamide group), the BW of the IV-treated group (Acrylamide – Hesperidin group) was not statistically significantly different (p = 0.053) (Table 1 and histogram 1).

Table (1): Showing comparison between the studied cases according to means ± SD of body weight in the four studied groups.

Weight (gm)	Group I (n = 10)	Group II (n = 10)	Group III (n = 10)	Group IV (n = 10)	Test of Sig.	P-value
Range	183.0-215.0	186.0-219.0	164.0-196.0	174.0-203.0	F= 7.76	<0.001*
Mean ± SD	196.80 ± 11.60	199.60 ± 11.19	177.40 ± 11.11	187.60 ± 11.69		
Post-hoc	p1=586, p2=0.001*, p3=0.080, p4<0.001*, p5=0.024*, p6<0.053					

Data are presented as frequency (%) unless otherwise mentioned, SD: Standard deviation.

p1: p-value for comparing group I and group II
p2: p-value for comparing group I and group III
p3: p-value for comparing group I and group IV
p4: p-value for comparing group II and group III
p5: p-value for comparing group II and group IV
p6: p-value for comparing group III and group IV

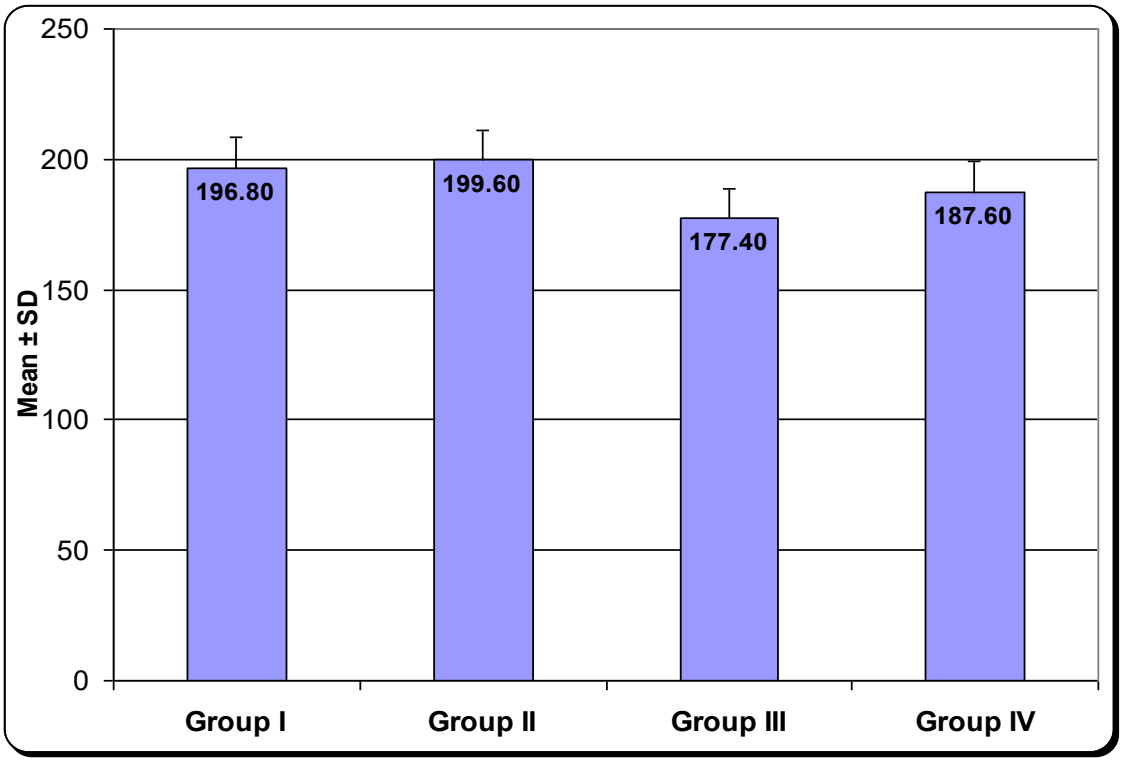

Histogram .1: Comparison between the studied cases according to means ± SD of body weight in the four studied groups.

Medial Prefrontal Cortex Thickness:

Comparing group III (the Acrylamide-treated group) to the control group I and group II (the Hesperidin-treated group), the medial prefrontal cortex thickness decreased statistically significantly (p=0,001). Comparing group IV (acrylamide–hesperidin) to group III (acrylamide-treated group), there was a statistically significant increase in medial PFC thickness (p=0,001). (Table 2 and Histogram 2).

Table (2): Showing comparison between the studied cases according to means ± SD of mPFC thickness in the studied groups.

The mPFC thickness (µm)	**Group I (n = 10)**	**Group II (n = 10)**	**Group III (n = 10)**	**Group IV (n = 10)**	**Test of Sig.**	**P-value**
Range.	981.9-1048.9	980.4-1045.6	867.4-970.6	929.3-1002.6	F=	<0.001*
Mean ± SD	1015.81 ± 24.12	1013.24 ± 23.91	910.83 ± 29.81	972.18 ± 26.36	35.15	
Post-hoc	p1=828, p2<0.001*, p3=0.001*, p4<0.001*, p5=0.001*, p6<0.001*					

Data are presented as frequency (%) unless otherwise mentioned, SD: Standard deviation.
p1: p-value for comparing group I and group II
p2: p-value for comparing group I and group III
p3: p-value for comparing group I and group IV
p4: p-value for comparing group II and group III
p5: p-value for comparing group II and group IV
p6: p-value for comparing group III and group IV

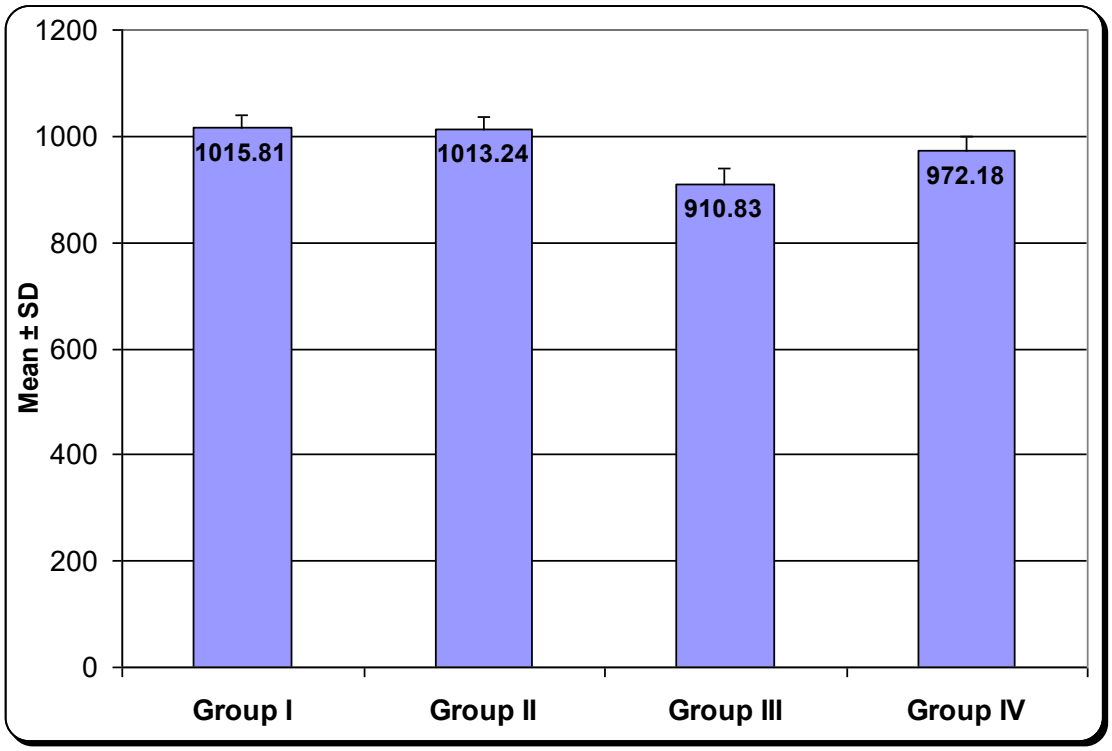

Histogram .2: Comparison between the studied cases according to means ± SD of mPFC thickness in the studied groups.

DISCUSSION

For many years, acrylamide (AC) has been widely used in wastewater treatment, soil conditioning, and the paper industry. In 1994, Ac was categorized as a class 2A drug by the International Agency for Research on Cancer (IARC), which stated that it was "most likely to cause cancer in humans" (Zhao *et al.,* 2022). Acrylamide leads to neurotoxic effects, reproductive and developmental issues, and certain tumors in animals. The impact of acrylamide on human health remains not completely understood (Çebi, 2024).

Since mice and rats resemble humans in terms of anatomy, physiology, and genetics, they have long been the preferred species for use as animal models in biomedical research. Rodents have several advantages, such as their short lifespan, abundance of genetic resources, low maintenance needs, and small size so we used rats in our research (Bryda, 2013). To avoid the effects of female hormones, including estrogen, which promote cellular proliferation throughout the cycle and lead to an increase in immature neurons in the cortex, the current study only utilized male albino rats (El-Safti *et al.,* 2017).

Our current investigation of the acrylamide-treated group's light microscopic examination revealed significant aberrant alterations in the medial prefrontal cortex's histological appearance with perivascular and cellular infiltration, shrunken pyramidal cells with strongly stained nuclei, pericellular halos, loss of processes, and uneven form. It also showed hemorrhage and congestion in both the pia mater and cortical blood vessels. The granule cells were damaged with ill-defined borders and lose of their nuclei. These outcomes were in accordance with (Farouk *et al.,* 2021) who observed comparable outcomes after giving rats a dose of AC at (25 mg/kg B.W. daily) and they attributed these changes to the production of ROS and an imbalance in antioxidants due to oxidative stress.

In our results examination of the semithin sections of the acrylamide–treated group of the fifth layer of medial prefrontal cortex revealed deformed, pyknotic, and deeply stained pyramidal cells with irregular cell bodies and axons.

Distorted granular cells with ill-defined borders, and loss of their nuclei. The obtained results were supported by a previous study done by (Mohamed, 2023), who found vacuolated cytoplasm and darkly pigmented nuclei. There were several neuroglial cells scattered among the nerve cells. myelin sheath disruption was observed in nerve fibers when he studied the acrylamide effect on the midbrain (Mohamed, 2023).

The ultrastructural findings of the acrylamide–treated group in our study showed that pyramidal cells appeared shrunken. The granular cells were also shrunken and showed nuclear membrane invagination and chromatin condensation. Our findings were consistent with the findings of (Mohamed, 2023) who observed that acrylamide induced ultrastructural alterations in the cells of the midbrain in the form of shrunken nuclei with an irregular nuclear membrane. The cytoplasm was rarified with ill-defined cell organelles and marked vacuolated areas. The nuclei showed peripheral chromatin condensation with marked invagination of the nuclear envelope. They had degenerated vacuolated cytoplasm. Some mitochondria were swollen and had disrupted cristae (Mohamed, 2023).

Our current study of immune histochemical stain reported an increase in the number and size of GFAP-positive cells in the acrylamide group as compared to the control group. These findings were in agreement with (Imam & Gadallah, 2019) ,who found that Ac groups exhibited the greatest GFAP expression and a greater number of positive cells that had long, branched cytoplasmic processes and an intense star shape (Imam & Gadallah, 2019). Findings of our immune histochemical results were also consistent with (Bouvier *et al* .,2022) as they linked astrocytic gliosis to an increase in GFAP activity, which thought to be a biomarker of neurotoxicity (Imam & Gadallah, 2019) .

Our results came in accordance with (Bhattacharyya *et al.,* 2014) who explained that the brain oxidative damage caused by Ac accumulation. ROS are essential for both cell signaling and homeostasis. ROS are known as ROS toxins or oxidative stressors because they can seriously harm cellular structures (Babizhayev, 2016). Furthermore, our findings in AC group could be also explained as toxicity may result in amino acids oxidation, damage to RNA or DNA, oxidative inactivation of certain enzymes, and the conversion of polyunsaturated fatty acids into lipids. These findings were in harmony with (Nita and Grzybowski , 2016).

A previous study done by (Foroutanfar *et al.,* 2020) illustrated that one mechanism stands for acrylamide-induced neurotoxicity is the apoptosis process as through the production of oxidative stress, acrylamide can readily break down the blood-brain barrier, penetrate brain cells, and initiate apoptotic pathways. Another research work indicated that AC may cause apoptosis of various neurocytes (Ünver *et al* ., 2020).

Scientists attributed the degeneration of nerve fibers observed in Ac intoxication to result from multiple mechanisms, including impaired axoplasmic transport, damage to the nucleus and mitochondria, inhibition of certain enzymes, and abnormalities in the synthesis of neuronal proteins (Kopanska *et al* .,2018).

In our present study of light microscopic examination showed that hesperidin apparently improved the harmful effects caused by acrylamide. These findings were in harmony with those of (Mandour *et al* .,2021) as they indicated that hesperidin administration had a positive effect on the prefrontal cortex's neurons. Our research results were also supported by (Balakrishnan & Menon, 2007) who demonstrated hesperidin's antioxidant activity against nicotine-induced neurotoxicity (Balakrishnan & Menon, 2007).

In agreement with our study, (Ishola *et al.,* 2021) showed that hesperidin pretreatment dramatically reduced oxidative damage and increased antioxidant enzyme activity in the cortex, hippocampal regions and striatum (Ishola *et al.,* 2021). In addition; hesperidin administration demonstrated the potential to treat spinal cord effects brought on by diabetes and bisphenol A indicating that hesperidin is one of a broad range of antioxidant supplements exhibited both inhibitory and therapeutic effectiveness against neurotoxicity caused by environmental pollutants and metabolic disorders (Yahyazadeh, 2024).

Comparing the acrylamide group to the control group in our morphometric study indicated a statistically significant decrease in body weight, which is in consistent with (Zhang *et al.,* 2020) finding that body weight considerably decreased following a 5-week exposure to acrylamide at a level of 20 mg/kg b.w. Our observations were also in line with (Hashem *et al.,*2022) as they outlined that a daily high dose of AC exposure causes oxidative stress to rise, which in turn causes a decreased rate of weight gain or a reduction in appetite. Furthermore, the AC's rapid reaction with amino and sulfhydryl residues in proteins, including cytoskeletal proteins, enzymes, and receptors that influence a range of biological processes. In this study the acrylamide–hesperidin treated group showed insignificant difference in the BW between acrylamide – hesperidin treated group and acrylamide group, and this observation were supported by (Mandour *et al.,* 2021) who used hesperidin in Alzheimer disease and found that here was an insignificant difference in the in-body weight compared to treated group (Mandour *et al.,* 2021).

In our investigation, the group that received acrylamide treatment had a statistically significant reduction in medial prefrontal cortex thickness when compared to the control group. These findings are consistent with those of (Amin *et al.,* 2019) who found that the acrylamide-treated group's external granular layer thickness was significantly less than that of the control group (Amin *et al.,* 2019).

Our study's acrylamide-hesperidin group demonstrated a statistically significant increase in mPFC thickness when compared to the acrylamide-treated group. This is consistent with (Mandour *et al.,* 2021) use of hesperidin in Alzheimer disease to show a significant increase in the thickness of the hippocampus's pyramidal cell layer and the prefrontal cortex (Mandour *et al.,* 2021).

Conclusion

The results of this study indicated that acrylamide negatively impact the histological appearance of the medial prefrontal cortex in rats and hesperidin administration can mitigate this acrylamide-induced brain damage.

Declarations:

Ethics Approval: Following the NIH guidelines for the Care and Use of Laboratory Animals and Faculty of Medicine's Ethics Committee Guidelines, with ethical permission number (17101763) Assiut University, Assuit, Egypt.

Conflict of Interest: The authors declare no conflict of interest.

Author contribution: Hala M. Hassanin: data interpretation, study design and preparation of the manuscript. Mohamed El-Badry Mohamed: data interpretation and revision of the manuscript. Reham R. Abd Elhafiz: data interpretation, study design and preparation of the manuscript. Noha A. Rashed: data interpretation, study design and preparation of the manuscript. All authors have read and agreed to the published version of the manuscript.

Data Availability Statement: Data is contained within the article.

Funding Information: This research received no external funding.

Acknowledgment: We acknowledge the support and the help presented by Faculty of Medicine, Assuit University, Assuit, Egypt where the study was carried out.

We also thank all people who helped in collecting, processing of samples.

REFERENCE

Abdel-aziz, H., Mekawy, N. H., and Ibrahem, N. E. (2019). Histological and immune-histochemical study on the effect of zinc oxide nanoparticles on cerebellar cortex of adult male albino rats. *Egyptian Journal of Histology,* 42(1): 23-34. DOI:10.21608/ ejh.2018.5113.1024.

Amin, W. E. S., Hegab, A. S., Ibrahim, A. A. S., & Mokhtar, H. E. (2019). Effect of acrylamide on development of cerebellum in albino rat. *Egyptian Journal of Histology,* 42(4), 798-814. DOI: 10.21608/ejh.2019.7866.1079

Babizhayev MA (2016). Generation of reactive oxygen species in the anterior eye segment. Synergistic codrugs of N-acetylcarnosine lubricant eye drops and mitochondria-targeted antioxidant act as a powerful therapeutic platform for the treatment of cataracts and primary open-angle gulcoma. *BBA Clinical* ,6:49–68 https://doi.org/10.1016/j. bbacli.2016.04.004

Balakrishnan, A., and Menon, V. P. (2007). Protective effect of hesperidin on nicotine induced toxicity in rats. *Indian Journal of Expermeental Biology,*45(2): 194-202.

Bhattacharyya A, Chattopadhyay R, Mitra S and Crowe SE (2014). Oxidative stress: an essential factor in the pathogenesis of gastrointestinal mucosal diseases. *Physiological reviews,* 94:329–354 https://doi.org/ 10. 1152/physrev.00040.2012

Bouvier, D. S., Fixemer, S., Heurtaux, T., Jeannelle, F., Frauenknecht, K. B., and Mittelbronn, M. (2022). The multifaceted neurotoxicity of astrocytes in ageing and age-related neurodegenerative diseases: a translational perspective. *Frontiers in Physiology,* 13: 814889- 81500. https://doi.org/ 10.3389/fphys. 2022.814889

Bryda, E. C. (2013). The Mighty Mouse: the impact of rodents on advances in biomedical research. *Missouri Medicine,* 110(3): 207-211.

Córcoles-Parada M, Müller NC, Ubero M, Serrano-Del-Pueblo VM, Mansilla F, Marcos-Rabal P, Artacho-Pérula E, Dresler M, Insausti R, Fernández G and M. Muñoz-López (2017). Anatomical segmentation of the human medial prefrontal cortex. *Journal of Comparitive Neurology;* 525:2376-2393. https://doi.org/ 10. 1002/ cne. 24212.

Çebi, A. (2024). Acrylamide intake, its effects on tissues and cancer. In *Acrylamide in food* (pp. 65-93). Academic Press. https:// doi.org/10.1016/B978-0-323-99119-3.00077-1

Elhelaly, A. E., AlBasher, G., Alfarraj, S., Almeer, R., Bahbah, E. I., Fouda, M. M., and Abdel-Daim, M. M. (2019). Protective effects of hesperidin and diosmin against acrylamide-induced liver, kidney, and brain oxidative damage in rats. *Environmental Science and Pollution Research;* 26: 35151-35162. https://doi.org/10.1007/ s11356-019-06660-3.

El-Safti F. E. N. A., El-Kholoy W. B., El-Mehi A. E. and Selima R. R. (2017). A comparative study on the effect of aging on the hippocampal CA1 area of male albino rat. *Menoufia Medical Journal,* 30(4): 1079 https://doi. org/10.4103/1110-2098.229200

Farouk, S. M., Gad, F. A., Almeer, R., Abdel-Daim, M. M., and Emam, M. A. (2021). Exploring the possible neuroprotective and antioxidant potency of lycopene

against acrylamide-induced neurotoxicity in rats' brain. *Biomedicine & Pharmacotherapy,* 138:111458-111470.

Foroutanfar, A., Mehri, S., Kamyar, M., Tandisehpanah, Z., and Hosseinzadeh, H. (2020). Protective effect of punicalagin, the main polyphenol compound of pomegranate, against acrylamide- induced neurotoxicity and hepato-toxicity in rats. *Phytotherapy Research,* 34(12): 3262-3272. https://doi.org/10.1002/ptr.6774

García-Cabezas, M. Á., Zikopoulos, B., and Barbas, H. (2019). The Structural Model: a theory linking connections, plasticity, pathology, development and evolution of the cerebral cortex. *Brain Structure and Function;* 224(3): 985-1008. https://doi. org/ 10. 1007/ s00429- 019-01841-9

Gedik, S., Erdemli, M.E., Gul, M., Yigitcan, B., Gozukara Bag, H., Aksungur, Z. and Altinoz, E. (2017). Hepatoprotective effects of crocin on biochemical and histopathological alterations following acrylamide -induced liver injury in Wistar rats. *Biomedcine Pharmacotherapy;* 95:764–770. https://doi.org/10.1016/j.biopha.2017.08.139.

Haghmorad, D., Mahmoudi, M. B., Salehipour, Z., Jalayer, Z., Rastin, M., Kokhaei, P., and Mahmoudi, M. (2017). Hesperidin ameliorates immunological outcome and reduces neuroinflammation in the mouse model of multiple sclerosis. *Journal of neuroimmunology;* 302: 23-33. https://doi. org/ 10. 1016/ j. jneuroim.2016.11.009.

Hashem, M. M., Abo-El-Sooud, K., Abd El-Hakim, Y. M., Badr, Y. A. H., El-Metwally, A. E., and Bahy-El-Dien, A. (2022). The impact of long-term oral exposure to low doses of acrylamide on the hematological indicators, immune functions, and splenic tissue architecture in rats. *International Immuno-pharmacology,* 105: 108568-108580. https://doi.org/10.1016/j.intimp.2022.108568

Heidbreder, C. A., and Groenewegen, H. J. (2003). The medial prefrontal cortex in the rat: evidence for a dorso-ventral distinction based upon functional and anatomical characteristics. *Neuroscience & BiobehavioralReviews;*27(6):555-579. https://doi.org/10.1016/j. neubiorev.2003.09.003

Imam R. A. and Gadallah H. N. (2019). Acrylamide-induced adverse cerebellar changes in rats: possible oligodendrogenic effect of omega 3 and green tea. *Journals Via Medica;* 78(3): 564-574. DOI: 10.5603/FM.a2018.0105

Ishola, I. O., Ben-Azu, B., Adebayo, O. A., Ajayi, A. M., Omorodion, I. L., Edje, K. E., and Adeyemi, O. O. (2021). Prevention and reversal of ketamine-induced experimental psychosis in mice by the neuroactive flavonoid, hesperidin: The role of oxidative and cholinergic mechanisms. *Brain research bulletin,* 177, 239-251. https://doi.org/10.1016/j.brainresbull.2021.10.007

Jung, U. J., and Kim, S. R. (2018). Beneficial effects of flavonoids against Parkinson's disease. *Journal of medicinal food;* 21(5): 421-432. https://doi.org/10.1089/jmf.2017.4078

Kolk, S. M., and Rakic, P. (2022). Development of prefrontal cortex. *Neuropsycho-pharmacology;* 47(1): 41-57.

https://doi.org/ 10.1038/s 41386-021-01137-9.

Kopanska, M., Muchacka, R., Czech, J., Batoryna, M., & Formicki, G. (2018). Acrylamide toxicity and cholinergic nervous system. *Journal of Physiology & Pharmacology:* 69(6): 847-858. DOI: 10.26402/jpp.2018.6.03.

Kosari-Nasab, M., Shokouhi, G., Ghorbanihaghjo, A., Abbasi, M. M., and Salari, A. A. (2018). Hesperidin attenuates depression -related symptoms in mice with mild traumatic brain injury. *Life sciences;* 213: 198-205. https://doi.org/10.1016/j. lfs.2018.10.040.

Küçükler, S., Çomaklı, S., Özdemir, S., Çağlayan, C., and Kandemir, F. M. (2021). Hesperidin protects against the chlorpyrifos-induced chronic hepatorenal toxicity in rats associated with oxidative stress, inflammation, apoptosis, autophagy, and upregulation of PARP-1/VEGF. *Environmental Toxicology;* 36(8): 1600-1617. https://doi. org/10.1002/tox.23156.

Mandour, D. A., Bendary, M. A., and Alsemeh, A. E. (2021). Histological and imuno-histochemical alterations of hippocampus and prefrontal cortex in a rat model of Alzheimer like-disease with a preferential role of the flavonoid "hesperidin". *Journal of Molecular Histology,* 52(5): 1043-1065. https://doi.org/10. 1007/ s10735-021-09998-6

Mohamed, H. Z. E. (2023). A Histological and Immuno-histochemically Study on the Possible Protective Action of Lithium Chloride on the Acrylamide Induced Toxicity During the Postnatal Development of Midbrain Red Nucleus in Male Albino Rats. *Egyptian Journal of Histology,* 46(2): 693-712. DOI: 10. 21608/ejh.2022.112840.1620.

Mohapatra, A. N., and Wagner, S. (2023). The role of the prefrontal cortex in social interactions of animal models and the implications for autism spectrum disorder. *Frontiers in Psychiatry*; *14*:103389-1205199. https://doi.org/10. 3389/fpsyt.2023.1205199.

Nita, M., & Grzybowski, A. (2016). The role of the reactive oxygen species and oxidative stress in the pathomechanism of the age-related ocular diseases and other pathologies of the anterior and posterior eye segments in adults. *Oxidative medicine and cellular longevity,* 2016(1): 3164734. https://doi.org/10. 1155/2016/3164734

Parhiz, H., Roohbakhsh, A., Soltani, F., Rezaee, R., and Iranshahi, M. (2015). Antioxidant and anti-inflammatory properties of the citrus flavonoids hesperidin and hesperetin: an updated review of their molecular mechanisms and experimental models. *Phytotherapy research;* 29(3): 323-331. https://doi.org/10. 1002/ptr.5256.

Park, J. S., Samanta, P., Lee, S., Lee, J., Cho, J. W., Chun, H. S., and Kim, W. K. (2021). Developmental and neuro-toxicity of acrylamide to zebrafish. *International Journal of Molecular Sciences;* 22(7): 3518-3530. https://doi.org/10. 3390/ijms22073518

Rifai, L., and Saleh, F. A. (2020). A review on acrylamide in food: Occurrence, toxicity, and mitigation strategies. *International Journal of Toxicology;*39(2): 93-102. https://doi.org/1 0.1177/ 1091581820 902405.

Roohbakhsh, A., Parhiz, H., Soltani, F., Rezaee, R., and Iranshahi, M. (2015). Molecular mechanisms

behind the biological effects of hesperidin and hesperetin for the prevention of cancer and cardiovascular diseases. *Life sciences;* 124: 64-74. https://doi.org/10.1016/j.lfs.2014.12.030.

Sabo, I. J. R., Lakic, T. Z., Capo, I. D., Andrejic-Visnjic, B. M., Matavulj, M., and Djolai, M. A. (2021). Effects of Acute Oral Exposure to Acrylamide on Histological Structures of the Stomach in Wistar Rats. *International Journal of Morphology;* 39(4): 963-968. http://dx.doi.org/10.4067/S0717-95022021000400963

Sawikr, Y., Yarla, N. S., Peluso, I., Kamal, M. A., Aliev, G., and Bishayee, A. (2017). Neuroinflammation in Alzheimer's disease: the preventive and therapeutic potential of polyphenolic nutraceuticals. *Advances in protein chemistry and structural biology;* 108: 33-57. https://doi.org/10.1016/bs.apcsb.2017.02.001.

Shukor, M. Y. (2019). Applications, Pollution, Toxicity and Bioremediation of Acrylamide. *Journal of Environmental Microbiology and Toxicology;* 7(2): 1-6. https://doi.org/10.54987/jemat.v7i2.489.

Suvarna, K. S., Layton, C., and Bancroft, J. D. (2018). Bancroft's theory and practice of histological techniques. Elsevier health sciences.

Turk, E., Kandemir, F. M., Yildirim, S., Caglayan, C., Kucukler, S., and Kuzu, M. (2019). Protective effect of hesperidin on sodium arsenite-induced nephrotoxicity and hepatotoxicity in rats. *Biological trace element research,* 189: 95-108. https://doi.org/10.1007/s12011-018-1443-6

Ünver Saraydin, S., Saraydin, D., & Şahin İnan, Z. D. (2020). A study of digital image analysis on the acrylamide derivative monomers induced apoptosis in rat cerebrum. *Microscopy research and technique,* 83(4): 436-445. https://doi.org/10.1002/jemt.23431

Woods, A. E., and Stirling, J. W. (2018). Transmission electron microscopy. *Bancroft's theory and practice of histological techniques:* 434-475.

Yahyazadeh, A. (2024). The effectiveness of hesperidin on bisphenol A-induced spinal cord toxicity in a diabetic rat model. *Toxicon*, *243*, 107724. https://doi.org/10.1016/j.toxicon.2024.107724

Zamani, E., Shokrzadeh, M., Ziar, A., Abedian-Kenari, S., and Shaki, F. (2018). Acrylamide attenuated immune tissues' function via induction of apoptosis and oxidative stress: Protection by l-carnitine. *Human & Experimental Toxicology,* 37(8): 859-869. https://doi.org/10.1177/0960327117741753

Zhang, L., Hara, S., Ichinose, H., Nagashima, D., Morita, K., Sakurai, T., and Ichihara, G. (2020). Exposure to acrylamide decreases noradrenergic axons in rat brain. *Neurotoxicology,* 78: 127-133. https://doi.org/10.1016/j.neuro.2020.03.001

Zhao, M., Zhang, B., and Deng, L. (2022). The mechanism of acrylamide- induced neurotoxicity: Current status and future perspectives. *Frontiers in nutrition;* (9),488-575: Article 859189. https://doi.org/10.3389/fnut.2022.859189.

Zouhairi, N., Kahloula, K., Adli Djallal Eddine, H., Abdelmohcine, A., Draoui, A., Chatoui, H., and Abdelali, B. (2022). Acrylamide, the Unnatural

Compound: Exposure and Toxicity on Humans and Animals. In Nutrition and Human Health: Effects and Environmental Impacts (Cham: Springer International Publishing: 325-341. https:// doi. org/10.1007/9.

ARABIC SUMMARY

الدور الوقائي المحتمل للهيسبيريدين مقابل التأثيرات العصبية السامة التي يسببها الأكريلاميد على القشرة الجبهية لدى ذكور الجرذان البيضاء البالغة

هالة محمد حسنين، محمد البدري محمد، ريهام رفعت عبد الحفيظ، نهى احمد راشد
قسم التشريح البشري و علم الأجنة، كلية الطب، جامعة أسيوط، مصر.

الخلفية: مع ظهور مادة الأكريلاميد في منتجاتنا اليومية، ظهرت العديد من الآثار الضارة.
الهيسبيريدين هو جليكوسيد فلافوني يستخدم عادة كعامل مضاد للالتهابات .
الهدف من هذا العمل: تقديم أساس تجريبي للوقاية من التسمم بالأكريلاميد وتقليل اثاره باستخدام الهيسبيريدين.
المواد وطرق البحث : قُسِّم 40 جرذًا أبيض بالغًا من الذكور إلى أربع مجموعات: المجموعة الاولي (المجموعة الضابطة), المجموعة الثانية (مجموعة الهيسبيريدين) والتي تلقت الهيسبيريدين بجرعة 10 ملغم/كغم من وزن الجسم يوميًا حيث أُذيب الهيسبيريدين في 0.1% كربوكسي ميثيل
سليلوز. المجموعة الثالثة (مجموعة الاكريلاميد) تلقت الاكريلاميد بجرعة 25 ملغم/كغم من وزن الجسم يوميًا، بينما المجموعة الرابعة (مجموعة الاكريلاميد والهيسبيريدين) تلقت الجرعات نفسها التي تلقتها المجموعتان الثانية والثالثة. أُعطيت جميع العلاجات عن طريق الفم عن طريق التغذية الأنبوبية لمدة 21 يومًا متتالية. في نهاية التجربة، استُخرجت قشور الفص الجبهي وعُولجت للفحص المجهري الضوئي والإلكتروني والصبغة المناعية الكيميائية. كما أُجريت قياسات مورفومترية.
النتائج: أظهرت المجموعة المعالجة بالاكريلاميد نزيفًا واحتقانًا في كل من الأوعية الدموية القشرية والأم الحنون مع تسلل خلوي ومحيط بالأوعية الدموية. تقلصت الخلايا الهرمية مع وجود هالات حول الخلايا، وفقدت نواتها. تأثرت الخلايا الحبيبية وأصبحت حدودها غير واضحة وفقدت نواتها. كشفت الدراسات المورفومترية عن انخفاض كبير في وزن الجسم وسمك قشرة الفص الجبهي الأمامي لدى الفئران. من ناحية أخرى، أظهرت الفئران التي تلقت الهيسبيريدين مع الأكريلاميد بنية طبيعية واضحة إلى حد ما.
الخلاصة: العلاج بالهيسبيريدين قادر على تخفيف تلف الدماغ الناجم عن الأكريلاميد لدى الفئران.

.

.